Inorg. Chem. **1994**, *33,* 1071–1079

Synthesis and X-ray Crystal Structures of a Calixarene-Related, Tetraamino, Tetraphenolic, Polynucleating Macrocyclic Ligand and Its Zn^{II}_4 and Co^{III}_3 Derivatives

Martin J. Grannas, Bernard F. Hoskins, and Richard Robson*

School of Chemistry, University of Melbourne, Parkville, Victoria 3052, Australia

Received July 30, 1993®

Reduction with $NaBH_4$ of the macrocyclic tetra Schiff base ligand formed by condensation of two molecules of 2,6-diformyl-4-methylphenol with two molecules of 2,6-bis(aminomethyl)-4-methylphenol affords the corresponding tetraamino, tetraphenolic macrocyclic ligand L_rH_4. Determination of the structure of the hydrochloride salt with the remarkable solvation composition $L_rH_4{\cdot}4HCl{\cdot}H_2O{\cdot}CH_3OH{\cdot}C_2H_5OH$, reveals a dome-shaped $L_rH_8^{4+}$ cation with a water molecule and two of the chloride ions H-bonded inside the domed macrocyclic cavity. Crystal data: monoclinic, space group $P2_1/c$, $a = 16.190(3)$ Å, $b = 10.246(3)$ Å, $c = 26.756(6)$ Å, $\beta = 96.88(2)°$, $Z = 4$. Reaction of $L_rH_4{\cdot}4HCl$ with zinc acetate in methanol containing tetraethylammonium hydroxide affords crystals of $[L_4Zn^{II}_4(OH)(CH_3CO_2)_3(CH_3OH)]{\cdot}1.5CH_3OH$ whose structure was determined by X-ray crystallography. Crystal data: monoclinic, space group $C2/c$, $a = 34.213(9)$ Å, $b = 16.028(3)$ Å, $c = 20.640(3)$ Å, $\beta = 119.17(2)°$, $Z = 8$. The macrocycle binds the four zincs in a kite-shaped arrangement totally lacking in symmetry. A central hydroxo ligand bridges three of the zincs and is 2.849(5) Å from the fourth zinc. Ignoring this weak interaction with the hydroxo, this fourth zinc has an irregular 4-coordinate geometry; two of the remaining zincs are 5-coordinate, and the other is 6-coordinate. Reaction in air of $L_rH_4{\cdot}4HCl$ with cobaltous acetate in the presence of OH^- and BF_4^- yields crystals of $[L_rCo^{III}_3(OH)(CH_3CO_2)_3]BF_4{\cdot}3.83H_2O$ whose structure was determined by X-ray crystallography. Crystal data: monoclinic, space group $P2_1/n$, $a = 15.555(3)$ Å, $b = 15.141(4)$ Å, $c = 21.723(3)$ Å, $\beta = 98.96(1)°$, $Z = 4$. The macrocycle binds three cobalt(III) centers, the fourth nucleation site being vacant. A central bridging hydroxo ligand and three bridging acetato ligands afford distorted octahedral arrangements for all three cobalts.

Introduction

The organization provided by an appropriately designed binucleating ligand can confer upon its derived binuclear complexes unusual structural features[1] and unusual reactivity, including catalytic properties, e.g., dipalladium complexes of certain binucleating ligands catalyze the hydration of nitriles to carboxamides by a bimetallic pathway.[2] Such complexes, moreover, provide useful models for certain proteins containing pairs of metal centers;[3] e.g., a dimanganese complex of a 2,6-diformyl-4-methylphenol-derived binucleating ligand was recently shown to act as a functional model for manganese-containing catalase.[4] The expectation that unique behavior may similarly be shown by complexes in which a single ligand organizes more than two metal centers into some predetermined arrangement has prompted us to study the synthesis and properties of complexes of macrocyclic ligands such as I[5] (hereafter L_sH_4) potentially capable of binding up to four metal centers in close proximity.

Although system I offers much scope for new chemistry, the more robust and more flexible tetraamine ligand II, which is the subject of the present report, may have significant advantages in a number of areas of potential application. For example, reactivity studies with complexes of II may be possible under conditions where analogous complexes of I could not be used because of degradative attack at the weak link in the ligand, namely, the imine. Moreover, a desirable feature of a polynuclear metal derivative which is intended to catalyze some sort of multistep reaction of substrates is sufficient flexibility to allow metal–metal spatial relationships and individual metal coordination geometries to vary from one intermediate to the next as substrates are first introduced, then suffer modification, and finally are expelled; the potentially more flexible system II may have distinct advantages over I in such applications.

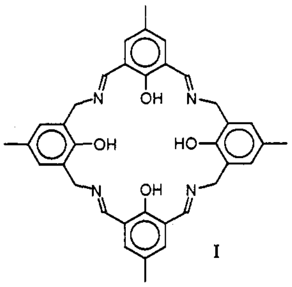
I

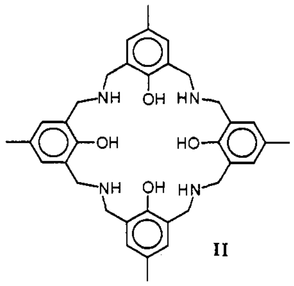
II

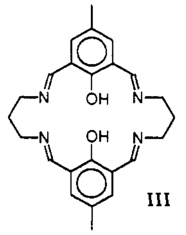
III

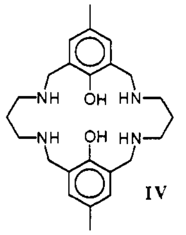
IV

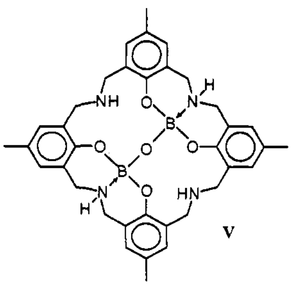
V

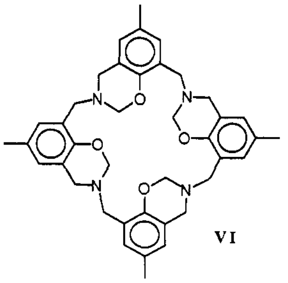
VI

With regard to differing redox chemistries of derived metal complexes, the pair of macrocycles III and IV provides a close

---

® Abstract published in *Advance ACS Abstracts,* February 15, 1994.

(1) Robson, R. *Inorg. Chim. Acta* **1982,** *57,* 71.
(2) McKenzie, C. J.; Robson, R. *J. Chem. Soc., Chem. Commun.* **1988,** 112.
(3) Fenton, D. E. In *Advances in Inorganic and Bioinorganic Mechanisms*; Sykes, A. G., Ed.; Academic Press Inc.: London, 1983; Vol. 2, p 187.
(4) Sakiyama, H.; Okawa, H.; Isobe, R. *J. Chem. Soc., Chem. Commun.* **1993,** 882.
(5) Bell, M.; Edwards, A. J.; Hoskins, B. F.; Kachab, E. H.; Robson, R. *J. Am. Chem. Soc.* **1989,** *111,* 3603. Edwards, A. J.; Hoskins, B. F.; Kachab, E. H.; Markiewicz, A.; Murray, K. S.; Robson, R. *Inorg. Chem.* **1992,** *31,* 3585.

0020-1669/94/1333-1071$04.50/0

parallel with **I** and **II**. Ligand **IV** apparently facilitates the attainment of a wider range of oxidation states in its binuclear derivatives than **III**.[6] For applications in the area of multielectron oxidation and reduction of substrates, therefore, **II** again promises advantages over **I**.

As a tetraphenolic macrocycle in which the phenolic nuclei are interconnected by the carbons ortho to the hydroxyl, **II** has much in common with the calixarenes which were intensively studied in recent years, having numerous actual and potential applications in the supramolecular area;[7] indeed, the cup-shaped structures of some of the derivatives of **II** described herein are very reminiscent of the calixarenes. Some examples of "enlarged" calixarenes in which the links between phenolic nuclei have been extended beyond the normal methylene and to which general class **II** belongs were recently studied.[8]

Reported here are the synthesis of **II** (hereafter L_rH_4) and some of its chelating chemistry, including the X-ray structural characterization of the tetrahydrochloride of the metal-free ligand ($L_rH_4{\cdot}4HCl$), a tetrazinc complex, and a tricobalt complex.

Results

$L_rH_4{\cdot}4HCl$. Reduction of a suspension of the orange dihydrochloride, $L_sH_4{\cdot}2HCl$,[2] of the tetra Schiff base ligand **I** in ethanol at 0 °C gave a suspension of an amorphous yellow solid which we found too insoluble in all solvents tested to allow recrystallization. Comparison of the IR spectrum of this crude solid with that of an authentic sample of L_rH_4 obtained from a subsequently obtained sample of pure $L_rH_4{\cdot}4HCl$ indicated that it consisted mainly of L_rH_4. The crude solid suspended in methanol dissolved upon treatment with HCl and analytically pure, crystalline $L_rH_4{\cdot}4HCl{\cdot}H_2O$ could be isolated from the solution so formed. The ^{1}H NMR spectrum of $L_4H_4{\cdot}4HCl$ in D_2O was very simple, showing only three singlets at δ 2.16, 4.14, and 7.07 in 3:4:2 proportions, arising from the methyl, methylene, and aromatic hydrogens respectively.

Single crystals suitable for X-ray crystallography with the remarkable solvation composition $L_rH_4{\cdot}4HCl{\cdot}H_2O{\cdot}CH_3OH{\cdot}C_2H_5OH$ were obtained by recrystallization from a mixture of methanol ("good" solvent) and ethanol ("poor" solvent) acidified with HCl gas. The methanol and ethanol were "undried", the small percentage of water contained therein providing the water molecule selectively trapped (as described below) at the center of the macrocycle. Crystal data and details of the crystal structure determination are given in Table 1.

Figure 1a shows a front view and the atom-numbering scheme, and Figure 1b shows a side view of the macrocyclic tetracation $L_rH_8{}^{4+}$ together with the associated four chloride ions and the water, methanol, and ethanol molecules which are involved in a complex hydrogen-bonded network. Atomic coordinates are given in Table 2, and selected interatomic distances and angles are given in Table 3.

The $L_rH_8{}^{4+}$ cation adopts a dome-shaped arrangement with all four phenolic oxygen atoms oriented toward the top of the dome and the aromatic methyl groups along its lower rim. The four nitrogen atoms are close to planar, the maximum deviation from the average N_4 plane being 0.14 Å. The four aromatic rings are inclined almost equally to this average N_4 plane, the dihedral angles falling in the narrow range 45.9–47.6°. Both hydrogens of each $NH_2{}^+$ are on the same side of the N_4 plane, the four hydrogens associated with N1 and N3 being on the side toward the top of the dome and those associated with N2 and N4 on the opposite side.

The macrocycle is deformed by internal hydrogen bonding so that the O1···O4 and O2···O3 separations are considerably less than the O1···O2 and O3···O4 separations. As is indicated in Figure 1a, O1 and O4 are hydrogen bonded to N1 [O1···N1, 2.841(14) Å; O4···N1, 2.802(11) Å] and likewise O2 and O3 are hydrogen bonded to N3 [O2···N3, 2.829(12) Å; O3···N3, 2.688(13) Å]. The hydrogens on N2 and N4 by contrast are not involved in hydrogen bonding to adjacent phenolic centers but rather to chloride and water.

Two of the chlorides, Cl3 and Cl4, and both the methanol and ethanol are located outside the $L_rH_8{}^{4+}$ dome whereas the water and the other two chlorides are inside. The water molecule is approximately centrally located within the macrocyclic cavity, being 0.37 Å "above" the N_4 plane and roughly the same distance "below" the group of four phenolic oxygens. Cl1 and Cl2 are simultaneously associated with the upper region of the dome of one macrocyclic system and with the interior of the dome above ($Cl1^{III}$ and $Cl2^{III}$). The two O–H bonds of the water molecule are H bonded to Cl1 above and $Cl2^{III}$ below. In addition the water oxygen atom is hydrogen bonded to the N–H of N4 and the O–H of the phenolic O3.

The hydrogen atoms associated with O1 and O4 were not observed in the crystal structure analysis, but the short distances between these oxygens and certain chlorides were strongly suggestive of hydrogen bonding [O1···Cl1, 3.036(10) Å; cl2···O4, 3.019(9) Å].

L_rB_2O. We routinely produce $L_sH_4{\cdot}2HCl$ as orange crystals by maintaining just below its boiling point a methanolic solution containing 2,6-diformyl-4-methylphenol and 2,6-bis(aminomethyl)-4-methylphenol and acetic acid; the crystals reproducibly start to separate after about 2 h. When a solution so obtained, just before $L_sH_4{\cdot}2HCl$ would be expected to appear, is cooled to ice temperature and treated with excess sodium borohydride, a colorless crystalline solid separates whose elemental composition is consistent with the formulation L_rB_2O (**V**). The parent peak isotopic pattern in the FAB mass spectrum centered at *m/e* 631 is consistent with this formulation (theoretical mass of L_rB_2O is 631.36). The insolubility of L_rB_2O prevented NMR spectra from being recorded. We were unable to obtain crystals of L_rB_2O suitable for X-ray studies.

L_rB_2O on treatment with HCl gave $L_rH_4{\cdot}4HCl$.

Incorporation of CH_2 Groups into the Nucleation Sites of L_4. Reaction of $L_rH_4{\cdot}4HCl$ with formaldehyde and lithium acetate in 1:4:8 proportions in methanol gives **VI**, characterized by elemental analysis, MS, and IR and NMR spectroscopy. The ^{1}H NMR spectrum was very simple, showing the aliphatic protons as four singlets and the aromatic protons as an AB quartet.

VI was readily hydrolyzed by aqueous ethanolic HCl to $L_rH_4{\cdot}4HCl$.

$L_rZn^{II}_4(OH)(CH_3CO_2)_3(CH_3OH)$. Reaction mixtures in boiling methanol of zinc acetate tetrahydrate, $L_4H_4{\cdot}4HCl{\cdot}H_2O$, lithium acetate dihydrate, and tetraethylammonium hydroxide in 5:1:10:10 proportions upon cooling gave colorless crystals of composition $[L_rZn^{II}_4(OH)(CH_3CO_2)_3(CH_3OH)]{\cdot}1.5CH_3OH$.[9] X-ray diffraction studies were carried out on a single crystal grown directly from such a reaction mixture.

The structure of the $L_rZn^{II}_4(OH)(CH_3CO_2)_3(CH_3OH)$ molecule and the atom-numbering scheme are represented in Figure 2. Atomic coordinates are given in Table 4, and selected interatomic distances and angles are given in Table 5. The complex is bowl-shaped but totally lacking in symmetry, being present in the crystal in enantiomeric pairs; in Figure 2 the view is down into the bowl. The four zincs are arranged in an unsymmetrical pattern resembling a kite with Zn1 at the most acute vertex, which has been bent from planarity around its short diagonal, Zn2···Zn4. The dihedral angle between the Zn1···

---

(6) Mandal, S. K.; Thompson, L. K.; Nag, K.; Charland, J.-P.; Gabe, E. J. *Can. J. Chem.* **1987**, *65*, 2815. Das, R.; Nag, K. *Inorg. Chem.* **1991**, *30*, 2831.

(7) McKervey, A.; Bohmer, V. *Chem. Br.* **1992**, 724.

(8) Okada, Y.; Kasai, Y.; Ishii, F.; Nishimura, J. *J. Chem. Soc., Chem. Commun.* **1993**, 976.

(9) Grannas, M. J.; Hoskins, B. F.; Robson, R. *J. Chem. Soc., Chem. Commun.* **1990**, 1644.

Table 1. Crystal Data Together with Details of the Data Collection and Structure Refinements for $L_rH_4{\cdot}4HCl{\cdot}H_2O{\cdot}CH_3OH{\cdot}C_2H_5OH$, $[L_rZn_4(OH)(CH_3CO_2)_3(CH_3OH)]{\cdot}1.5CH_3OH$, and $[L_rCo_3(OH)(CH_3CO_2)_3]BF_4{\cdot}3.83H_2O$

	compd		
	$L_rH_4{\cdot}4HCl{\cdot}H_2O{\cdot}CH_3OH{\cdot}C_2H_5OH$	$[L_rZn^{II}_4(OH)(CH_3CO_2)_3(CH_3OH)]{\cdot}1.5CH_3OH$	$[L_rCo^{III}_3(OH)(CH_3CO_2)_3]BF_4{\cdot}3.83H_2O$
formula	$C_{39}H_{60}Cl_4N_4O_7$	$C_{43}H_{54}N_4O_{12}Zn_4{\cdot}1.5CH_4O$	$C_{42}H_{50}BCo_3F_4N_4O_{11}{\cdot}3.83H_2O$
fw	838.7	1128	1119.5
descrptn of cryst	colorless prism	colorless parallelepiped	brown monotruncated octahedron
cryst system	monoclinic	monoclinic	monoclinic
space group	$P2_1/c$ (No. 14)	$C2/c$ (No. 15)	$P2_1/n$ (No. 14)
a, Å	16.190(3)	34.213(9)	15.555(3)
b, Å	10.246(3)	16.028(3)	15.141(4)
c, Å	26.756(6)	20.640(3)	21.723(3)
β, deg	96.88(2)	119.17(2)	98.96(1)
V, Å^3	4406(3)	9883(8)	5054(3)
Z	4	8	4
ρ(calcd), g cm^{-1}	1.243	1.516	1.475
ρ(measd), g cm^{-1}	1.27(1)	1.47(1)	1.53(1)
temp, K	293(1)	293(1)	293(1)
radiation (λ, Å)		Mo Kα, graphite monochromator (0.710 69)	
no. of int control reflns	3 measd every 9000 s; no significant variation	3 measd every 4800 s; no significant variation	3 measd every 3600 s; no significant variation
F(000)	1784	4664	2310
cryst dimens (dist in mm from point within cryst)	±(001), 0.038; ±(010), 0.288; ±(100), 0.063	±(100), 0.100; ±($1\bar{1}0$), 0.113; ±($10\bar{1}$), 0.200	±(001), 0.150; ±($10\bar{1}$), 0.093; ±(110), 0.157; ±($1\bar{1}0$), 0.136; ($\bar{1}\bar{1}2$), 0.143
μ, cm^{-1}	2.72	20.0	10.5
transm factors (SHELX-76)	min 0.963, max 0.980	min 0.565, max 0.735	min 0.734, max 0.832
2θ limits, deg	$2 \le 2\theta \le 45$	$2 \le 2\theta \le 45$	$2 \le 2\theta \le 45$
hlk limits			
h	$-2 \to 17$	$0 \to 29$	$-1 \to 16$
k	$0 \to 11$	$0 \to 10$	$0 \to 16$
l	$-28 \to 28$	$-24 \to 24$	$-23 \to 23$
scan mode	$\omega/2\theta$	$\omega/2\theta$	$\omega/2\theta$
instrument		Enraf-Nonius CAD-4F diffractometer	
no. of reflns measd	7415	8196	7828
no. of unique reflns	5736	6457	6608
R_{int}	0.0136	0.026	0.018
no. of unique reflns used	2234 [$I > 2.5\sigma(I)$]	4171 [$I > 2.5\sigma(I)$]	4596 [$I > 2\sigma(I)$]
refinement	full-matrix least squares	blocked full-matrix least squares	blocked full-matrix least squares
function minimized		$\sum w\Delta^2$, where $\Delta = \lVert F_o\rvert - \lvert F_c \rVert$ (SHELX-76)	
weighting scheme	$w = k/[\sigma F^2 + gF^2]$	$w = k/[\sigma F^2 + gF^2]$	unit weights
g	0.00065	0.0017	
k	1.924	1.410	
final R [$=\sum\lvert\Delta\rvert/\sum\lvert F_o\rvert$]	0.076	0.046	0.076
final R_w [$=\sum w^{1/2}\lvert\Delta\rvert/\sum w^{1/2}\lvert F_o\rvert$]	0.072	0.044	
max shift/esd for non-H atoms	0.024	0.03	0.109 (U_{iso} of B1; max cation shift/esd = 0.005)
max resid electron density, e Å^{-3}	0.73	0.42	1.09

Zn2···Zn4 and the Zn3···Zn2···Zn4 planes is 39.3°. The "diagonal" Zn···Zn separations are 5.111(2) Å for Zn1···Zn3 and 3.468(1) Å for Zn2···Zn4.

Each Zn is bound to L_r^{4-} by two phenolate oxygens and one nitrogen. An approximately centrally located hydroxide is strongly coordinated to Zn2 [2.029(3) Å] and Zn4 [2.012(5) Å], less strongly to Zn3 [2.267(5) Å], and weakly if at all to Zn1 [2.849(5) Å]. An acetate on the concave surface of the bowl bridges Zn2 and Zn4. A monodentate acetate completes the coordination sphere of Zn1 which has an irregular 4-coordinate geometry if the weak interaction with the central hydroxo ligand is ignored. Zn2 is of pseudooctahedral geometry with a coordinated methanol *trans* to the bridging acetate oxygen (O1AB). Zn3 with a monodentate acetate has an irregular 5-coordinate geometry intermediate between square pyramidal and trigonal bipyramidal; using the criterion τ for trigonality of 5-coordinate centers,[10] according to which a square pyramidal geometry has $\tau = 0$ and a trigonal bipyramidal geometry has $\tau = 1$, Zn3 with $\tau = 0.41$ approximates to neither. Zn4 is 5-coordinate, being bonded to two phenolates and one nitrogen of L_r, to the central hydroxide, and to an oxygen of the bridging acetate; its geometry approximates to square pyramidal ($\tau = 0.10$) with the acetato O2AB occupying the apical position.

The conformation of the macrocycle is such that N1–H and N3–H are directed outward from the molecular bowl and N2–H and N4–H are directed toward the inside of the bowl. In keeping with the bowl-like structure of the molecule, the four aromatic rings are all inclined on the same side of the average N_4 plane, the dihedral angles to that plane being 30.1, 46.9, 24.7, and 39.0° for the 100, 200, 300, and 400 rings, respectively.

^{13}C and ^1H NMR spectra of a freshly dried sample of the tetrazinc complex in $CDCl_3$ are consistent with the presence of solution species undergoing rapid interconversion so as to produce an averaged arrangement with C_{2v} symmetry, as shown in Figure 3, where the atom labeling used in the discussion below is shown. These interconversions render the four methylenes g, g′, g″, g‴ equivalent, the other four methylenes i, i′, i″, i‴ equivalent to each other but different from the g methylenes, the four aromatic nuclei equivalent, and the two monodentate acetates equivalent.

In the ^1H NMR spectrum, the bridging acetate methyl (l) produces a 3H singlet at δ 0.97, and the two monodentate acetate methyls (m) produce a 6H singlet at δ 2.05. The four ligand methyl groups (a) give rise to a 12H singlet at δ 2.18. The aromatic protons (c and d) of four equivalent rings generate an AB quartet (δ 6.76, 6.86; J = 2.3 Hz). Two broad peaks at δ 2.55 and 3.06

---

(10) Addison, A. W.; Rao, T. N.; Reedjik, J.; van Rijn, J.; Verschoor, G. C. *J. Chem. Soc., Dalton Trans.*, **1984**, 1349.

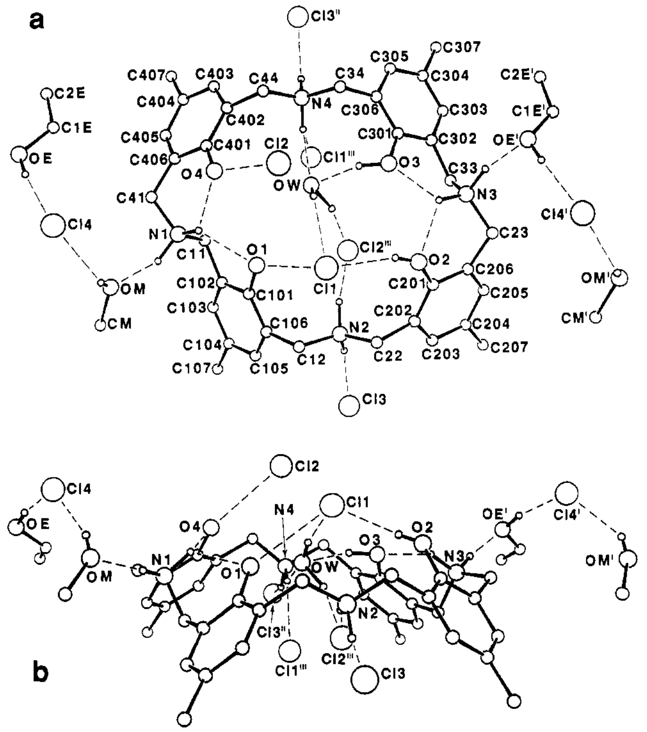

Figure 1. Front view (a) and side view (b) of $L_rH_8^{4+}$ with the associated Cl^-, H_2O, CH_3OH, and C_2H_5OH, showing the atom-numbering scheme. Hydrogen bonds are indicated by thin dashed lines. Symmetry codes: **I**, $x - 1, y, z$; **II**, $-x, 1^1/_2 + y, -^1/_2 - z$; **III**, $-x, ^1/_2 + y, ^1/_2 - z$.

Table 2. Final Atomic Coordinates and Equivalent Isotropic Displacement Parameters (Å^2) for $L_rH_4{\cdot}4HCl{\cdot}H_2O{\cdot}CH_3OH{\cdot}C_2H_5OH$ (Esd Values in Parentheses)

atom	x	y	z	U_{eq}[a]
Cl1	0.0142(2)	0.8541(3)	0.1838(1)	0.0444(8)
Cl2	0.0441(2)	0.2536(4)	0.1949(1)	0.0470(9)
Cl3	0.0035(2)	0.2662(4)	−0.0051(1)	0.052(1)
Cl4	0.5022(3)	0.8243(4)	0.2407(2)	0.084(1)
O1	0.1348(6)	0.5340(8)	0.3160(3)	0.042(2)
O2	−0.1890(6)	0.4656(8)	0.3143(3)	0.039(2)
O3	−0.1561(5)	0.5336(9)	0.1967(3)	0.038(2)
O4	0.1847(5)	0.4485(8)	0.2003(3)	0.036(2)
N1	0.2880(6)	0.5759(9)	0.2766(3)	0.030(2)
N2	−0.0110(6)	0.6101(9)	0.4050(3)	0.027(2)
N3	−0.2987(6)	0.5787(9)	0.2359(3)	0.030(2)
N4	0.0040(6)	0.5991(9)	0.1124(3)	0.027(2)
C101	0.1653(8)	0.6202(12)	0.3532(5)	0.035(2)
C102	0.2270(8)	0.7056(12)	0.3409(4)	0.030(2)
C103	0.2624(8)	0.7943(12)	0.3761(5)	0.038(2)
C104	0.2392(10)	0.7986(13)	0.4238(5)	0.045(2)
C105	0.1786(8)	0.7164(12)	0.4358(4)	0.038(2)
C106	0.1413(8)	0.6275(12)	0.4015(4)	0.031(2)
C107	0.2818(10)	0.8944(13)	0.4629(4)	0.056(2)
C11	0.2514(9)	0.7070(11)	0.2874(4)	0.038(2)
C12	0.0718(8)	0.5412(11)	0.4162(4)	0.029(2)
C201	−0.2096(9)	0.5592(12)	0.3440(5)	0.032(2)
C202	−0.1653(8)	0.5953(12)	0.3897(5)	0.032(2)
C203	−0.1942(8)	0.6976(11)	0.4184(4)	0.029(2)
C204	−0.2672(8)	0.7635(12)	0.4024(4)	0.033(2)
C205	−0.3125(8)	0.7247(12)	0.3575(4)	0.038(2)
C206	−0.2837(8)	0.6244(12)	0.3280(4)	0.031(2)
C207	−0.2997(9)	0.8715(13)	0.4339(5)	0.054(2)
C22	−0.0866(9)	0.5268(12)	0.4115(4)	0.038(2)
C23	−0.3398(8)	0.5778(13)	0.2834(4)	0.037(2)
C301	−0.1806(9)	0.6225(12)	0.1597(4)	0.034(2)
C302	−0.2456(8)	0.7059(12)	0.1678(5)	0.032(2)
C303	−0.2779(8)	0.7895(12)	0.1298(4)	0.035(2)
C304	−0.2461(8)	0.7924(12)	0.0837(5)	0.034(2)
C305	−0.1815(8)	0.7105(13)	0.0764(5)	0.039(2)
C306	−0.1473(8)	0.6213(12)	0.1136(4)	0.032(2)
C307	−0.2828(9)	0.8857(12)	0.0439(5)	0.050(2)
C33	−0.2737(8)	0.7123(12)	0.2188(4)	0.052(2)
C34	−0.0794(8)	0.5302(11)	0.1028(4)	0.032(2)
C401	0.2046(8)	0.5452(12)	0.1689(5)	0.032(2)
C402	0.1560(9)	0.5759(13)	0.1225(4)	0.036(2)
C403	0.1864(8)	0.6737(12)	0.0926(4)	0.028(2)
C404	0.2604(8)	0.7393(13)	0.1060(4)	0.033(2)
C405	0.3037(8)	0.7077(11)	0.1517(4)	0.027(2)
C406	0.2788(8)	0.6120(12)	0.1828(4)	0.031(2)
C407	0.2919(8)	0.8427(13)	0.0717(4)	0.045(2)
C41	0.3324(8)	0.5751(13)	0.2296(4)	0.036(2)
C44	0.0742(8)	0.5092(12)	0.1053(5)	0.037(2)
OW	−0.0057(5)	0.0531(8)	0.2797(3)	0.041(2)
OM	0.4303(7)	0.5037(9)	0.3383(4)	0.079(3)
CM	0.4771(15)	0.589(2)	0.3878(8)	0.186(5)
OE	0.5725(7)	0.4574(10)	0.1732(4)	0.079(3)
C1E	0.5124(14)	0.533(2)	0.1407(8)	0.133(5)
C2E	0.525(2)	0.581(2)	0.0974(9)	0.206(5)
H1W	−0.027(5)	0.618(6)	0.250(4)	0.142(6)
H2W	0.000(5)	0.486(6)	0.233(4)	0.142(6)
HO2	−0.146(4)	0.441(5)	0.308(3)	0.017(6)
HO3	−0.097(4)	0.527(5)	0.199(3)	0.017(6)
H1M	0.4389(-)	0.4407(-)	0.3305(-)	0.142(6)
H1E	0.5548(-)	0.4066(-)	0.1980(-)	0.142(6)

[a] $U_{eq} = {}^1/_3\sum_i\sum_j[U_{ij}(a^*_i a^*_j)(\vec{a}_i{\cdot}\vec{a}_j)]$.

assigned to two sorts of N–H disappear upon D_2O exchange. The methylenes appear as complex multiplets as a result of coupling to NH superimposed on the geminal coupling, but these signals simplify upon D_2O exchange to two AB quartets, one widely spaced (δ 3.45, 4.42, 8H; J = 11.6 Hz) and the other closely spaced (δ 3.95, 3.98; J = 12.8 Hz).

The particularly simple ^{13}C NMR spectrum is consistent with the above rapid interconversion to generate an averaged arrangement with C_{2v} symmetry: δ 20.05, four equivalent methyls (a); δ 22.7, 23.09 in roughly 1:2 proportions, methyls of bridging acetate (l) and two monodentate acetates (m), respectively; δ 52.50 and 54.25, almost same height, two different types of methylenes (g and i); δ 122.6, carbon para to phenolic O in all four equivalent aromatic nuclei (b); δ 124.6 and 125.1, carbons ortho to phenol (e/f); δ 131.1 and 131.4, meta carbons (c/d); δ 159.6, ipso carbons (h); δ 179.6 and 179.1 in roughly 1:2 proportions, carboxylate carbons of bridging acetate (k) and the two monodentate acetates (n, n′), respectively.

The averaged C_{2v} arrangement apparent in the spectra is consistent with the bridging acetate inside the bowl remaining bound to the same pair of zincs throughout the interconversions, thereby preventing the bowl from turning inside out. Rapid exchange of the "central" hydroxide between a position considerably closer to Zn3 than to Zn1 (as in Figure 2) and an analogous position closer to Zn1 than to Zn3 together with conformational flexing of L_r renders Zn1 equivalent to Zn3, Zn2 equivalent to Zn4, all four methylenes, g, g′, g″, g‴ equivalent, and so on.

$[L_rCo^{III}_3(OH)(CH_3CO_2)_3]BF_4$. In initial attempts to isolate a polycobalt complex of L_r free of chloride, crude L_rH_4 was first converted to presumed $L_rH_4{\cdot}4HBF_4$ (uncharacterized) by concentrating a solution to which HBF_4 had been added. When a suspension of this salt in hot water was treated with methanolic solutions of cobaltous acetate, tetraethylammonium hydroxide, and tetrabutylammonium tetrafluoroborate in approximately 1:5:10:5 proportions, the suspended salt dissolved and a small amount of dirty pink solid remained undissolved. The latter was removed by filtration, and the filtrate was concentrated and allowed to cool. Black platelike crystals separated over a period of several days. The crystals after being dried in vacuum and then exposed to the atmosphere had an elemental composition consistent with the formulation $[L_rCo^{III}_3(OH)(CH_3CO_2)_3]BF_4{\cdot}5H_2O$ whereas an X-ray crystallographic analysis of a crystal sealed with mother liquor indicated the presence of 3.83 H_2O. Crystals suitable for X-ray studies were obtained by slow diffusion in air of water vapor into a reaction mixture in methanol containing the presumed $L_rH_4{\cdot}4HBF_4$ and 5 equiv of cobaltous acetate. After the structural study was complete, it was found that chloride did not in fact

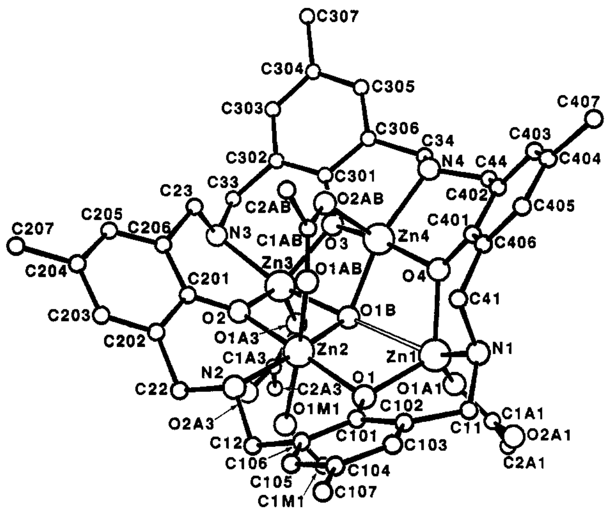

Figure 2. Structure and atom-numbering scheme for $[L_rZn^{II}_4(OH)(CH_3CO_2)_3(CH_3OH)]$.

Table 3. Selected Interatomic Distances (Å) and Angles (deg) for $L_rH_4{\cdot}4HCl{\cdot}H_2O{\cdot}CH_3OH{\cdot}C_2H_5OH$

	Distances[a]		
Cl1···O1	3.036(10)	Cl4···OE	3.049(12)
Cl1···O2	3.047(10)	O1···N1	2.841(14)
$Cl1^{III}$···N4	3.229(9)	O2···N3	2.829(12)
Cl1···OW	3.243(9)	O3···N3	2.688(13)
Cl2···O4	3.019(9)	O3···OW	2.628(11)
$Cl2^{III}$···N2	3.041(9)	O4···N1	2.802(11)
$Cl2^{III}$···OW	3.234(9)	N1···OM	2.769(14)
$Cl2^{II}$···N4	3.175(9)	N3···OE^{I}	2.805(14)
Cl4···OM	3.097(12)	N4···OW	2.922(11)
phenolic C–O	1.31(2)–1.377(15)	arom C–C	1.34(2)–1.42(2)
N–C	1.49(2)–1.52(2)	other C–C	1.48(2)–1.54(2)
	Angles		
C–N–C	111.5(8)–115.0(8)	C–C–C angle at arom C's	116.8(9)–123.4(9)
C–C–N	108.8(8)–114.2(9)		

[a] Symmetry codes: I, $x - 1, y, z$; II, $-\bar{x}, 1^1/_2 + y, -^1/_2 - z$; III, $-x, ^1/_2 + y, ^1/_2 - z$.

interfere and that the same product could be obtained more straightforwardly using L_rH_4C4HCl without conversion to the BF_4^- salt.

The X-ray analysis revealed that the asymmetric unit consists of $[L_rCo^{III}_3(OH)(CH_3CO_2)_3]^+$ cations, a BF_4^- anion distributed over two sites, and water of solvation. Two views of the cation and the atom-numbering scheme are given in Figure 4. Atomic coordinates are given in Table 6, and selected interatomic distances and angles are given in Table 7.

The cation adopts a saddle-shaped conformation with three Co(III) ions in a triangular arrangement [Co1···Co2, 2.851(2) Å; Co1···Co3, 3.369(3) Å; Co2···Co3, 2.804(2) Å]. The fourth nucleation site provided by L_r^{4-} is vacant. Each of the three metals is essentially octahedral, the macrocyclic ligand providing two phenolate oxygen donors and one amine nitrogen donor to each, meridional at Co1 and Co3 and facial at Co2. A pyramidal μ_3-hydroxide is almost equidistant from the three cobalts and is 0.667 Å below the Co_3 plane. Two acetate coligands on the same side of the Co_3 plane as the hydroxide bridge from Co1 to Co2 and from Co3 to Co2 such that they are *cis* at Co2. A third μ_2-acetate on the opposite side of the Co_3 plane bridges from Co1 to Co3 so the two acetates bound to each of these centers are *trans* to each other. The hydrogens of the three coordinating amines are mutually *syn* on the same side of the Co_3 plane as the hydroxide. The two bridging phenoxide oxygen centers, O1 and O2, are markedly pyramidal [sums of bond angles 338(2) and 336(2)°, respectively] as can be seen in Figure 4.

Table 4. Final Atomic Coordinates and Equivalent Isotropic Displacement Parameters (Å^2) for $[L_rZn_4(OH)(CH_3CO_2)_3(CH_3OH)]{\cdot}1.5CH_3OH$ (Esd Values in Parentheses)

atom	*x*	*y*	*z*	U_{eq}[a]
Zn1	0.13648(3)	0.03837(6)	0.47442(5)	0.0402(2)
Zn2	0.18468(3)	0.06356(6)	0.65007(4)	0.0402(2)
Zn3	0.10832(3)	0.12158(5)	0.68720(5)	0.0383(2)
Zn4	0.09470(3)	0.19085(6)	0.53861(5)	0.0475(2)
O1	0.19174(14)	0.0037(3)	0.5649(2)	0.038(1)
O2	0.17420(14)	0.1151(3)	0.7324(2)	0.040(1)
O3	0.06722(14)	0.1998(3)	0.6083(2)	0.041(1)
O4	0.11049(15)	0.1532(3)	0.4597(2)	0.042(1)
N1	0.16580(2)	0.0612(4)	0.4119(3)	0.042(1)
N2	0.2517(2)	0.0446(4)	0.7274(3)	0.039(1)
N3	0.1149(2)	0.2029(4)	0.7712(3)	0.038(1)
N4	0.0486(2)	0.2785(4)	0.4654(3)	0.040(1)
O1B	0.11751(13)	0.0808(3)	0.5903(2)	0.036(1)
O1A1	0.0876(2)	–0.0334(4)	0.4608(3)	0.057(1)
O2A1	0.1046(2)	–0.0993(4)	0.3850(3)	0.068(1)
C1A1	0.0815(3)	–0.0920(5)	0.4149(4)	0.053(2)
C2A1	0.0453(3)	–0.1536(6)	0.4014(6)	0.097(2)
O1A3	0.0649(2)	0.0387(4)	0.6831(3)	0.065(1)
O2A3	0.1200(2)	–0.0435(4)	0.7546(3)	0.066(1)
C1A3	0.0802(3)	–0.0242(6)	0.7225(4)	0.054(2)
C2A3	0.0487(3)	–0.0787(6)	0.7349(6)	0.100(2)
O1AB	0.20232(15)	0.1775(3)	0.6205(3)	0.050(1)
O2AB	0.1473(2)	0.2684(3)	0.5952(3)	0.048(1)
C1AB	0.1873(3)	0.2490(5)	0.6135(4)	0.051(2)
C2AB	0.2188(3)	0.3189(6)	0.6270(8)	0.143(3)
O1M1	0.1688(2)	–0.0610(3)	0.6890(3)	0.054(1)
C1M1	0.1506(3)	–0.1339(6)	0.6466(5)	0.091(2)
C101	0.2328(2)	–0.0039(4)	0.5689(4)	0.037(2)
C102	0.2383(2)	–0.0018(5)	0.5062(4)	0.039(2)
C103	0.2811(2)	–0.0063(5)	0.5153(4)	0.045(2)
C104	0.3195(2)	–0.0162(5)	0.5827(4)	0.046(2)
C105	0.3125(2)	–0.0227(5)	0.6429(4)	0.043(2)
C106	0.2707(2)	–0.0180(4)	0.6378(4)	0.038(2)
C107	0.3653(2)	–0.0215(6)	0.5902(5)	0.073(2)
C11	0.2006(2)	–0.0021(5)	0.4279(4)	0.043(2)
C12	0.2672(2)	–0.0313(5)	0.7071(4)	0.046(2)
C201	0.2056(2)	0.1548(4)	0.7933(4)	0.034(2)
C202	0.2493(2)	0.1207(5)	0.8295(4)	0.036(1)
C203	0.2824(2)	0.1615(5)	0.8912(4)	0.042(2)
C204	0.2746(2)	0.2332(5)	0.9194(4)	0.045(2)
C205	0.2308(2)	0.2631(5)	0.8844(4)	0.043(2)
C206	0.1968(2)	0.2265(5)	0.8224(4)	0.036(2)
C207	0.3112(3)	0.2761(6)	0.9880(4)	0.063(2)
C22	0.2586(2)	0.0393(5)	0.8046(4)	0.042(2)
C23	0.1506(2)	0.2643(5)	0.7856(4)	0.041(2)
C301	0.0470(2)	0.2691(5)	0.6148(4)	0.043(2)
C302	0.0518(2)	0.2949(4)	0.6839(4)	0.036(2)
C303	0.0310(2)	0.3692(5)	0.6851(4)	0.045(2)
C304	0.0053(2)	0.4181(5)	0.6235(5)	0.047(2)
C305	–0.0007(2)	0.3893(5)	0.5559(4)	0.045(2)
C306	0.0189(2)	0.3158(5)	0.5502(4)	0.040(2)
C307	–0.0160(3)	0.4988(5)	0.6276(5)	0.067(2)
C33	0.0718(2)	0.2425(5)	0.7525(4)	0.042(2)
C34	0.0090(2)	0.2829(5)	0.4758(4)	0.048(2)
C401	0.1096(2)	0.2066(5)	0.4082(4)	0.037(2)
C402	0.0736(2)	0.2604(5)	0.3710(4)	0.040(2)
C403	0.0719(3)	0.3131(5)	0.3167(4)	0.047(2)
C404	0.1056(3)	0.3152(5)	0.2984(4)	0.051(2)
C405	0.1412(3)	0.2615(5)	0.3351(4)	0.051(2)
C406	0.1442(2)	0.2086(5)	0.3909(4)	0.044(2)
C407	0.1024(3)	0.3697(6)	0.2358(5)	0.075(2)
C41	0.1830(2)	0.1480(5)	0.4267(4)	0.044(2)
C44	0.0349(2)	0.2570(5)	0.3864(4)	0.046(2)
O1S1	0.1139(2)	0.4275(5)	0.5540(4)	0.095(2)
C1S1	0.1083(3)	0.4739(7)	0.6073(5)	0.085(3)
O1S2[b]	–0.0272(4)	0.0813(8)	0.0388(6)	0.069(3)
C1S2[b]	0.0006(7)	0.0349(11)	0.0112(11)	0.081(4)

[a] $U_{eq} = {}^1/_3\sum_i\sum_j[U_{ij}(a^*_ia^*_j)(\vec{a}_i\vec{a}_j)]$. [b] Site occupancy = 0.50.

The halves of the molecule on opposite sides of the average plane through N2, Co2, OB, C1A3, C2A3, and N4 have identical connectivities. As can be seen in Figure 4a this plane approximates to a mirror plane although the inequivalence of, for example, C12 and C22 is immediately apparent in this view. In the crystal,

Table 5. Selected Interatomic Distances (Å) and Angles (deg) for $[L_rZn_4(OH)(CH_3CO_2)_3(CH_3OH)]\cdot 1.5CH_3OH$ (Esd Values In Parentheses)

	Distances		
Zn1···Zn2	3.193(1)	Zn3···Zn4	3.076(2)
Zn1···Zn3	5.111(2)	Zn3–O2	1.978(5)
Zn1···Zn4	3.408(2)	Zn3–O3	1.992(4)
Zn1–O1	1.982(3)	Zn3–N3	2.092(7)
Zn1–O4	2.002(5)	Zn3–O1B	2.267(5)
Zn1–N1	2.017(8)	Zn3–O1A3	1.964(7)
Zn1···O1B	2.849(5)	Zn4–O3	2.072(6)
Zn1–O1A1	1.934(7)	Zn4–O4	2.041(5)
Zn2···Zn3	3.198(2)	Zn4–N4	2.103(6)
Zn2···Zn4	3.468(1)	Zn4–O1B	2.012(5)
Zn2–O1	2.117(5)	Zn4–O2AB	2.025(5)
Zn2–O2	2.072(5)	O1–C101	1.372(9)
Zn2–N2	2.081(5)	O2–C201	1.350(7)
Zn2–O1B	2.029(4)	O3–C301	1.349(10)
Zn2–O1AB	2.105(6)	O4–C401	1.353(10)
Zn2–O1M1	2.313(6)	O1M1–C1M1	1.410(10)
	Angles		
O1–Zn1–O4	123.4(2)	O1B–Zn3–O1A3	101.2(3)
O1–Zn1–N1	96.3(3)	O3–Zn4–O4	163.9(2)
O1–Zn1–O1A1	109.3(3)	O3–Zn4–N4	91.0(3)
O4–Zn1–N1	93.4(3)	O3–Zn4–O1B	83.3(2)
O4–Zn1–O1A1	103.7(3)	O3–Zn4–O2AB	97.7(3)
N1–Zn1–O1A1	132.8(3)	O4–Zn4–N4	91.2(3)
O1B–Zn1–O1A1	74.3(3)	O4–Zn4–O1B	88.8(2)
O1–Zn2–O2	175.6(3)	O4–Zn4–O2AB	97.8(3)
O1–Zn2–N2	92.4(3)	N4–Zn4–O1B	158.1(3)
O1–Zn2–O1B	96.4(2)	N4–Zn4–O2AB	98.6(3)
O1–Zn2–O1AB	89.3(3)	O1B–Zn4–O2AB	103.1(3)
O1–Zn2–O1M1	92.2(3)	Zn1–O1–Zn2	102.3(3)
O2–Zn2–N2	89.7(3)	Zn1–O1–C101	124.1(4)
O2–Zn2–O1B	81.2(2)	Zn2–O1–C101	121.2(4)
O2–Zn2–O1AB	94.6(3)	Zn2–O2–Zn3	104.3(3)
O2–Zn2–O1M1	84.0(3)	Zn2–O2–C201	125.0(4)
N2–Zn2–O1B	169.9(3)	Zn3–O2–C201	128.4(4)
N2–Zn2–O1AB	89.1(3)	Zn3–O3–Zn4	98.4(2)
N2–Zn2–O1M1	88.0(3)	Zn3–O3–C301	128.9(4)
O1B–Zn2–O1AB	96.1(3)	Zn4–O3–C301	123.7(4)
O1B–Zn2–O1M1	86.6(3)	Zn1–O4–Zn4	114.9(3)
O1AB–Zn2–O1M1	176.8(3)	Zn1–O4–C401	122.6(4)
O2–Zn3–O3	127.4(2)	Zn4–O4–C401	121.8(4)
O2–Zn3–N3	90.2(3)	Zn2–O1B–Zn3	96.1(2)
O2–Zn3–O1B	77.6(2)	Zn2–O1B–Zn4	118.3(3)
O2–Zn3–O1A3	130.5(3)	Zn3–O1B–Zn4	91.7(2)
O3–Zn3–N3	91.9(3)	Zn1–O1A1–C1A1	111.2(5)
O3–Zn3–O1B	78.8(2)	Zn3–O1A3–C1A3	116.9(6)
O3–Zn3–O1A3	99.9(3)	Zn2–O1AB–C1AB	132.6(5)
N3–Zn3–O1B	154.9(3)	Zn4–O2AB–C1AB	123.2(5)
N3–Zn3–O1A3	103.3(3)	Zn2–O1M1–C1M1	127.4(6)

the complex cation is buckled into an asymmetric conformation, both enantiomeric forms being present as is required by the centrosymmetric $P2_1/n$ space group. Some indication of the extent of the buckling from C_s symmetry is given by the inclinations to the Co_3 plane of the normals to the aromatic rings (C100 ring, 26.5°; C200 ring, 16.7°; C300 ring 60.2°; C400 ring, 55.7°).

^1H and ^{13}C NMR spectra in CD_3OD are consistent with the presence in solution of the two enantiomorphic conformers seen in the crystal structure undergoing rapid interconversion by ligand flexing so as to generate an averaged conformation with C_s symmetry. In CD_3OD solution, amino protons and methylene protons are decoupled so that the four different types of methylenes appear in the ^1H spectrum as four AB quartets (δ 3.34, 3.52, J = 13.5 Hz; δ 3.61, 4.09, J = 14.5 Hz; δ 3.75, 4.95, J = 12.0 Hz; δ 4.46, 4.50, J = 8.3 Hz); likewise, four singlets of methylene origin are seen in the ^{13}C NMR spectrum (δ 51.74, 52.57, 52.78, 54.40). All six carbons within any aromatic ring are inequivalent, so the effective C_s symmetry requires twelve different aromatic carbon atoms, all of which are seen in the ^{13}C NMR spectrum (δ 123.49, 124.63, 124.94, 125.67, carbons ortho to phenols; δ 127.77, 130.50, para carbons; δ 130.89, 131.28, 132.06, 132.66, meta carbons; δ 151.99, 159.12, ipso carbons). Likewise, in the ^1H NMR spectrum, essentially four singlets arising from the meta C–H's are seen (components from meta coupling not resolved). Consistent with the averaged C_s symmetry, two different types of ligand methyls are apparent in the ^1H NMR spectrum (δ 2.22, 2.24), but in the ^{13}C NMR spectrum, the two signals are superimposed (δ 20.20). Two different types of acetate

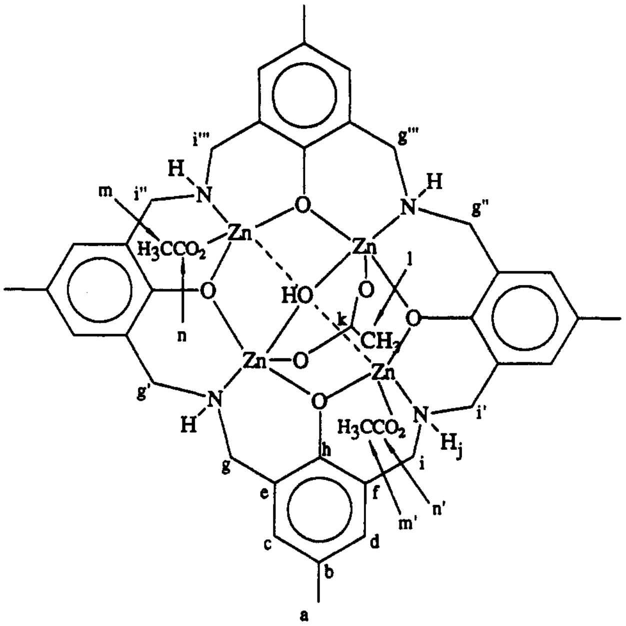

Figure 3. Averaged arrangement with C_{2v} symmetry of $[L_rZn^{II}_4(OH)(CH_3CO_2)_3]$ in solution including the NMR-labeling scheme.

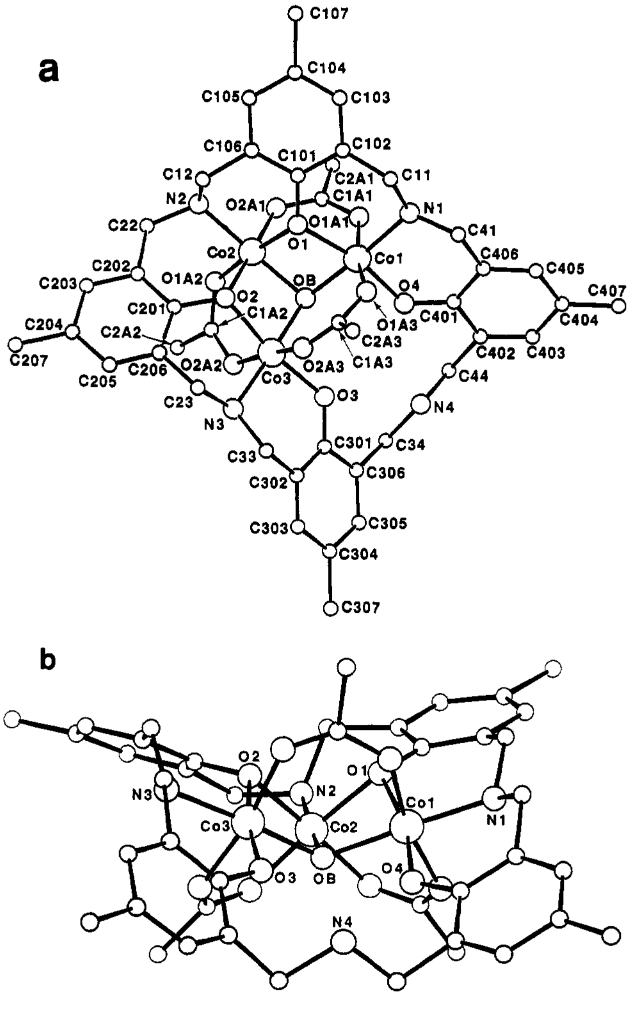

Figure 4. Front view (a) and side view (b) of the $[L_4Co^{III}_3(OH)(CH_3CO_2)_3]^+$ cation present in $[L_rCo^{III}_3(OH)(CH_3CO_2)_3]BF_4\cdot 3.83H_2O$.

Table 6. Final Atomic Coordinates and Equivalent Isotopic Displacement Parameters (Å^2) for the Atoms of the Cation in $[L_rCo_3(OH)(CH_3CO_2)_3]BF_4{\cdot}3.83H_2O$ (Esd Values in Parentheses)

atom	*x*	*y*	*z*	U_{eq}[a]
Co1[b]	0.17480(11)	0.46275(10)	0.21614(7)	0.0310(4)
Co2[c]	–0.00749(11)	0.43710(10)	0.21271(7)	0.0331(4)
Co3[d]	0.03996(12)	0.58274(11)	0.29030(7)	0.0401(4)
Co4[e]	0.1678(6)	0.4514(6)	0.3547(4)	0.042(2)
O1	0.0693(5)	0.4690(5)	0.1542(3)	0.036(2)
O2	–0.0452(5)	0.5558(5)	0.2171(3)	0.041(2)
O3	0.1330(6)	0.5911(6)	0.3560(4)	0.058(2)
O4	0.2575(5)	0.4647(5)	0.2882(4)	0.048(2)
N1	0.2594(6)	0.4384(7)	0.1602(4)	0.047(2)
N2	–0.1066(6)	0.4064(6)	0.1507(4)	0.042(2)
N3	–0.0183(7)	0.6879(7)	0.3145(5)	0.053(2)
N4	0.2964(8)	0.5329(7)	0.4080(5)	0.067(3)
O1B	0.0895(5)	0.4756(5)	0.2681(3)	0.039(2)
O1A1	0.1696(5)	0.3368(5)	0.2220(4)	0.043(2)
O2A1	0.0253(5)	0.3175(5)	0.2120(4)	0.042(2)
C1A1	0.1030(9)	0.2886(8)	0.2174(6)	0.042(3)
C2A1	0.1155(9)	0.1919(8)	0.2204(8)	0.070(3)
O1A2	–0.0694(5)	0.4052(5)	0.2765(4)	0.045(2)
O2A2	–0.0269(6)	0.5203(5)	0.3417(4)	0.051(2)
C1A2	–0.0700(9)	0.4492(9)	0.3264(6)	0.052(3)
C2A2	–0.1272(10)	0.4156(11)	0.3713(7)	0.078(3)
O1A3	0.1963(6)	0.5830(5)	0.2002(4)	0.049(2)
O2A3	0.0940(6)	0.6603(5)	0.2403(4)	0.048(2)
C1A3	0.1542(10)	0.6515(8)	0.2079(6)	0.048(3)
C2A3	0.1803(10)	0.7329(8)	0.1750(6)	0.060(3)
C101	0.0641(8)	0.4299(8)	0.0978(5)	0.040(2)
C102	0.1383(8)	0.4124(9)	0.0700(5)	0.047(3)
C103	0.1266(9)	0.3708(9)	0.0120(6)	0.053(3)
C104	0.0469(10)	0.3486(9)	–0.0191(6)	0.053(3)
C105	–0.0265(9)	0.3712(9)	0.0066(6)	0.050(3)
C106	–0.0183(8)	0.4123(9)	0.0645(6)	0.047(3)
C107	0.0405(11)	0.3013(11)	–0.0827(7)	0.079(3)
C11	0.2248(9)	0.4554(12)	0.0947(6)	0.072(3)
C12	–0.0994(8)	0.4450(9)	0.0892(5)	0.048(3)
C201	–0.1310(8)	0.5764(9)	0.2159(6)	0.045(2)
C202	–0.1997(9)	0.5200(8)	0.1927(6)	0.044(3)
C203	–0.2852(9)	0.5481(10)	0.1938(6)	0.057(3)
C204	–0.3049(10)	0.6296(10)	0.2188(6)	0.058(3)
C205	–0.2349(10)	0.6842(9)	0.2402(6)	0.057(3)
C206	–0.1502(9)	0.6604(9)	0.2389(6)	0.051(3)
C207	–0.3979(10)	0.6569(12)	0.2219(8)	0.089(3)
C22	–0.1901(8)	0.4263(9)	0.1696(6)	0.049(2)
C23	–0.0794(9)	0.7230(9)	0.2606(6)	0.051(3)
C301	0.1401(9)	0.6473(8)	0.4042(6)	0.050(3)
C302	0.0980(10)	0.7281(9)	0.4024(6)	0.059(3)
C303	0.1089(10)	0.7828(9)	0.4528(7)	0.059(3)
C304	0.1637(10)	0.7605(10)	0.5071(7)	0.061(3)
C305	0.2083(9)	0.6819(10)	0.5081(6)	0.058(3)
C306	0.1958(9)	0.6239(9)	0.4587(6)	0.051(3)
C307	0.1743(12)	0.8197(12)	0.5640(6)	0.083(3)
C33	0.0425(10)	0.7588(9)	0.3431(6)	0.065(3)
C34	0.2421(10)	0.5378(10)	0.4622(7)	0.065(3)
C401	0.3426(9)	0.4585(8)	0.2920(6)	0.051(3)
C402	0.3917(9)	0.4513(11)	0.3521(6)	0.064(3)
C403	0.4818(10)	0.4438(11)	0.3594(8)	0.079(3)
C404	0.5292(9)	0.4445(10)	0.3109(7)	0.061(3)
C405	0.4793(8)	0.4501(8)	0.2544(6)	0.052(3)
C406	0.3911(8)	0.4575(8)	0.2414(6)	0.046(2)
C407	0.6248(9)	0.4364(12)	0.3250(8)	0.081(3)
C41	0.3449(9)	0.4774(12)	0.1751(7)	0.072(3)
C44	0.3401(11)	0.4473(10)	0.4060(7)	0.080(3)

[a] $U_{eq} = {}^1/_3\sum_i\sum_j[U_{ij}(a^*_i a^*_j)(\vec{a}_i.\vec{a}_j)]$. [b] SOF = 0.935(5). [c] SOF = 0.958(5). [d] SOF = 0.972(5). [e] SOF = 0.174(5).

in 1:2 proportions are revealed [^{1}H NMR δ 2.12 (3H), 1.78 (6H); ^{13}C NMR δ 26.17 (methyl of acetate straddling pseudomirror plane), 24.05 (methyl of two equivalent acetates), 191.16, 191.22 (carboxylate)].

Discussion

$L_rH_4{\cdot}4HCl$. There has been considerable recent interest in anion-receptor systems;[11] the incorporation of the two chlorides inside the macrocyclic cavity of $L_rH_8^{4+}$ suggests that the general anion-binding properties of this carbon could be a worthwhile area for future study. Functionalization of L_rH_4 of the sort being currently intensively investigated with calixarenes[12] and cyclodextrins[13] promises to be easy and subject to wide variation; new systems for studies in the supramolecular area could thereby be provided.

Table 7. Selected Interatomic Distances (Å) and Angles (deg) for $[L_rCo_3(OH)(CH_3CO_2)_3]BF_4{\cdot}3.83H_2O$ (Esd Values in Parentheses)

	Distances		
Co1···Co2	2.851(2)	Co2–N2	1.939(9)
Co1···Co3	3.369(3)	Co2–O1B	1.870(7)
Co1–O1	1.956(7)	Co2–O2A1	1.882(8)
Co1–O4	1.865(8)	Co2–O1A2	1.870(9)
Co1–N1	1.960(10)	Co3–O2	1.948(7)
Co1–O1B	1.881(8)	Co3–O3	1.872(8)
Co1–O1A1	1.914(8)	Co3–N3	1.945(11)
Co1–O1A3	1.893(8)	Co3–O1B	1.890(8)
Co2···Co3	2.804(2)	Co3–O2A2	1.893(9)
Co2–O1	1.936(8)	Co3–O2A3	1.884(9)
Co2–O2	1.898(8)	OB–HB	0.962(7)
	Angles		
O1–Co1–O4	166.4(4)	O1–Co2–O2A1	92.2(4)
O1–Co1–N1	98.9(4)	O1–Co2–O1A2	173.0(4)
O1–Co1–OB	79.2(4)	O2–Co2–N2	92.5(4)
O1–Co1–O1A1	93.1(4)	O2–Co2–OB	84.1(4)
O1–Co1–O1A3	88.9(4)	O2–Co2–O2A1	176.4(4)
O4–Co1–N1	94.7(4)	O2–Co2–O1A2	90.5(4)
O4–Co1–OB	87.3(4)	N2–Co2–OB	174.8(4)
O4–Co1–O1A1	89.5(4)	N2–Co2–O2A1	87.2(4)
O4–Co1–O1A3	91.1(4)	N2–Co2–O1A2	90.4(4)
N1–Co1–OB	174.7(4)	OB–Co2–O2A1	96.5(4)
N1–Co1–O1A1	83.9(4)	OB–Co2–O1A2	93.5(4)
N1–Co1–O1A3	85.0(4)	O2A1–Co2–O1A2	85.9(4)
OB–Co1–O1A1	91.3(4)	O2–Co3–O3	169.5(4)
OB–Co1–O1A3	99.9(4)	O2–Co3–N3	96.1(5)
O1A1–Co1–O1A3	168.9(4)	O2–Co3–OB	82.2(4)
O1–Co2–O2	91.4(4)	O2–Co3–O2A2	90.6(4)
O1–Co2–N2	96.2(4)	O2–Co3–O2A3	88.1(4)
O1–Co2–OB	80.0(4)	O3–Co3–N3	94.4(5)

L_rB_2O. The formation of cyclic benzoxaborines when Schiff bases of salicylaldehyde derivatives are reduced by borohydride has been reported previously.[14] Molecular models suggest that the structure with boron in diagonally opposite nucleation sites of L_r (as in V) is much more likely than the alternative with boron in adjacent sites which contains a strained four-membered B_2O_2 ring. We have now characterized by X-ray crystallography[15] a number of binuclear derivatives of L_r^{4-} with metals in the diagonally opposite nucleation sites of the type proposed here for L_rB_2O.

Incorporation of CH_2 Groups into the Nucleation Sites of L_r. We had two reasons for studying the reaction between L_rH_4 and formaldehyde. The first was mere curiosity as to how many of the nucleation sites could be occupied by carbon centers. The second relates to the observation that L_rH_4 or some convenient derivative thereof is potentially very easily accessible by Mannich-related condensation of the inexpensive and readily available starting materials *p*-cresol, formaldehyde, and ammonia. Many attempts to generate L_r derivatives in this way under a variety of conditions have so far given only complex mixtures of products. VI appeared to be a likely outcome of these condensations, and this was one of the reasons for our attempting its synthesis, but

---

(11) Beer, P. D.; Dickson, C. A. P.; Fletcher, N.; Goulden, A. L.; Grieve, A.; Hodacova, J.; Wear, T. *J. Chem. Soc., Chem. Commun.* **1993**, 828.

(12) Arduini, A.; Casnati, A.; Fabbi, M.; Minari, P.; Pochini, A.; Sicuri, A. R.; Ungaro, R. In *Supramolecular Chemistry*; Balzini, V., Decola, L., Eds.; NATO ASI Series; Kluwer Academic Publishers: Dordrecht, The Netherlands, 1992; p 31.

(13) Kahn, A. R.; Barton, L.; D'Souza, V. T. *J. Chem. Soc., Chem. Commun.* **1992**, 1112.

(14) Andrews, P. R.; Gulbis, J. M.; Iskander, M. N.; Mackay, M. F. *Aust. J. Chem.* **1987**, *40*, 1073.

(15) Gable, R. W.; Grannas, M. J.; Hoskins, B. F.; Robson, R.; Rosenbaum, R. Unpublished results.

spectroscopic comparison of the product mixtures with authentic VI indicated it was not present.

$L_rZn^{II}_4(OH)(CH_3CO_2)_3(CH_3OH)$. The bizarre combination of geometrical features shown by $L_rZn^{II}_4(OH)(CH_3CO_2)_3(CH_3OH)$ is strikingly similar, although not identical in all details, to that shown by the analogous Zn_4 complex of the tetra Schiff base macrocycle $L_sZn_4(OH)(CH_3CO_2)_3$.[5] The central unsymmetrical $Zn_4(\mu\text{-}OH)(\mu\text{-}CH_3CO_2)$ systems present in both cases are almost identical with two short Zn–OH bonds, a third somewhat longer, and a fourth longer still. Moreover, the peculiar combination of metal coordination geometries *viz.* one 6-coordinate, two 5-coordinate, and one 4-coordinate is almost identical in the two cases. The most significant difference is that the acetate attached to the zinc most remote from the hydroxide (i.e. Zn1 in the present case) bridges on the convex side of the bowl to a neighboring Zn in the L_s case but is monodentate in the present case, the neighbor (Zn2) taking on instead a methanol ligand.

$[L_rCo^{III}_3(OH)(CH_3CO_2)_3]BF_4$. We note that the dimensions of the vacant nucleation site of L_r in this tricobalt complex seem appropriate for the incorporation of a range of metal cations to generate heterometallic clusters of potential interest. It is noteworthy that only three Co^{III} centers are incorporated under these conditions, but it is quite possible that under other conditions tetracobalt complexes of L_r could be obtained. Perhaps the failure to incorporate four Co^{III} centers is in some way related to the very strong preference of this d^6 cation for octahedral geometry. We have already identified a number of examples in which L_r incorporates only two metal centers, even in the presence of excess metal ion {e.g. $[(L_rH_2)(V^V_2O_3)H_2O]^{2+}$, $[(L_rH_2)Mo^{VI}_2O_5]$, and $[(L_rH_2)W^{VI}_2O_5]$}.[15]

Experimental Section

$L_rH_4 \cdot 4HCl$. Sodium borohydride (1.379 g, 36.5 mmol) was added in small portions to a stirred suspension of finely ground $L_sH_4 \cdot 2HCl$[5] (4.825 g, 7.293 mmol) in ice-cold ethanol (200 mL). The color changed gradually from orange to pale yellow. After the suspension had been stirred at 0 °C for 4 h, it was brought to the boil for 30 min. After the mixture had been cooled, the solid was collected, washed with water and ethanol, and then air-dried. A stirred suspension of the crude solid in cold methanol (150 mL) was acidified with a stream of HCl gas until the suspended solid dissolved. HCl was bubbled in for a further 5 min. The almost colorless solution was filtered and the filtrate concentrated by boiling at atmospheric pressure until a white solid appeared. Ethanol (120 mL) was added, and the flask was allowed to stand at room temperature overnight. The microcrystalline colorless solid was collected, washed with ethanol, and air-dried. Yield: 4.417 g, 79%. Drying the solid in vacuum at 80 °C for 2 h and subsequent exposure to the atmosphere produced a sample with composition $L_4H_4 \cdot 4HCl \cdot H_2O$. Anal. Calcd for $C_{36}H_{50}Cl_4N_4O_5$: C, 56.9; H, 6.4; Cl, 18.6; N, 7.4. Found: C, 57.2; H, 6.7; Cl, 18.3; N, 7.6.

L_rB_2O (V). A solution of 2,6-bis(aminomethyl)-4-methylphenol hydrochloride (1.013 g, 5.0 mmol) and acetic acid (0.150 g, 2.5 mmol) in hot methanol (75 mL) was added to a hot solution of 2,6-diformyl-4-methylphenol (0.821 g, 5.0 mmol) in methanol (50 mL) to produce a clear orange-yellow solution, which was maintained at 60 °C for 2 h. The solution was then quickly cooled to 0 °C, and sodium borohydride (1.890 g, 50 mmol) was added in small portions. The solution turned colorless, and when the evolution of H_2 had ceased, it was filtered and the filtrate was concentrated by boiling until solid began to separate. Upon cooling, colorless crystals of L_rB_2O formed, which were collected, washed with methanol, and dried in air. Yield: 46%. Anal. Calcd for $C_{36}H_{40}B_2N_4O_5$: C, 68.6; H, 6.4; B, 3.4; N, 8.9. Found: C, 68.7; H, 6.5; B, 3.1; N, 8.8.

Hydrolysis of L_rB_2O. Gaseous HCl was passed into a suspension of L_rB_2O (60 mg, 0.095 mmol) in methanol (20 mL) until almost all the solid had dissolved. The solution was filtered, and the filtrate was concentrated to a volume of approximately 10 mL by boiling at atmospheric pressure. Ethanol (30 mL) was added, and boiling was continued until solid began to separate. The colorless crystals which separated after the solution had been allowed to stand overnight were collected, washed with ethanol, and dried in air. Yield of $L_rH_4 \cdot 4HCl \cdot H_2O$, identified by IR: 57 mg, 79%.

Formaldehyde Condensation Product VI. To a solution of $L_rH_4 \cdot 4HCl \cdot H_2O$ (0.250 g, 0.329 mmol) in methanol (50 mL) at room temperature were added aqueous formaldehyde (0.133 g, 37% w/w, 1.64 mmol) and a solution of lithium acetate dihydrate (0.268 g, 2.63 mmol) in methanol (15 mL). A colorless, feathery, crystalline solid started to separate within minutes. After the reaction mixture had been standing overnight, the solid was collected, washed with ethanol, and dried in air. Yield: 0.147 g, 67%. Anal. Calcd for $C_{36}H_{44}N_4O_4$: C, 74.5; H, 6.9; N, 8.7. Found: C, 74.6; H, 7.0; N, 8.6.

Hydrolysis of VI. A sample of VI (50 mg, 0.78 mmol) suspended in ethanol (15 mL) dissolved upon addition of aqueous HCl (2 mL, 32% w/w). The solution was heated to boiling for 10 min and then evaporated to dryness under reduced pressure. The residue was triturated with ethanol, collected, washed with a little further ethanol, and dried in air, yielding $L_rH_4 \cdot 4HCl \cdot H_2O$ (40 mg, 68%), identified by its IR spectrum.

$[L_rZn^{II}_4(OH)(CH_3CO_2)_3] \cdot 2.5H_2O$. Near-boiling solutions of zinc acetate dihydrate (0.720 g, 3.28 mmol) in methanol (75 mL), lithium acetate dihydrate (0.670 g, 6.55 mmol) in methanol (50 mL), and tetraethylammonium hydroxide (3.09 g of 25% w/w solution in methanol, 5.24 mmol) were added to a solution of $L_rH_4 \cdot 4HCl \cdot H_2O$ (0.500 g, 0.66 mmol) in boiling methanol (75 mL). The resulting colorless solution was concentrated by boiling at atmospheric pressure to *ca.* 60 mL and allowed to stand at room temperature for 3 days, during which time clear colorless crystals separated which were shown by X-ray crystallography to have the composition $[L_rZn^{II}_4(OH)(CH_3CO_2)_3(CH_3OH)] \cdot 1.5CH_3OH$. The crystals were collected, washed with methanol, and dried in vacuum at 80 °C. Exposure to the atmosphere gave the hydrated material $[L_rZn^{II}_4(OH)(CH_3CO_2)_3] \cdot 2.5H_2O$. Yield: 0.507 g, 92%. Anal. Calcd for $C_{42}H_{55}N_4O_{13.5}Zn_4$: C, 46.1; H, 5.1; N, 5.1; Zn, 23.9. Found: C, 46.2; H, 5.1; N, 5.1; Zn, 24.2.

$[L_rCo^{III}_3(OH)(CH_3CO_2)_3]BF_4 \cdot xH_2O$ was prepared in two different ways. **Method 1: Via the Tetrafluoroborate Salt of $L_rH_8^{4+}$.** A suspension of crude L_rH_4 (0.910 g) in methanol (200 mL) to which aqueous HBF_4 (5 mL, 40%) had been added was heated to its boiling point. The resulting slightly fluorescent pale yellow-green solution was filtered at its boiling point, and the colorless filtrate was concentrated by boiling until a white precipitate started to separate. After 2 days at room temperature, the solid which had separated was collected, washed with methanol, and dried. Yield: 0.382 g. A suspension of a portion of this solid (0.290 g) in hot methanol (120 mL) containing cobaltous acetate tetrahydrate (0.374 g, 1.50 mmol) was heated under reflux for 30 min. The resulting brown solution was filtered while hot, and the filtrate was concentrated by boiling at atmospheric pressure to *ca.* 20 mL. Crystalline hydrated $[L_rCo^{III}_3(OH)(CH_3CO_2)_3]BF_4$ was obtained by slow transfer of water vapor in an enclosed chamber to the solution over a period of 20 days. Yield: 0.174 g. Drying the solid in vacuo at 80 °C for 2 h followed by re-exposure to the atmosphere gave a solid of composition $[L_rCo^{III}_3(OH)(CH_3CO_2)_3]BF_4 \cdot 5H_2O$. Anal. Calcd for $C_{42}H_{60}BCo_3F_4N_4O_{16}$: C, 44.2; H, 5.3; F, 6.7; N, 4.9. Found: C, 44.2; H, 5.3; F, 6.7; N, 4.9.

Method 2: Via $L_rH_4 \cdot 4HCl \cdot H_2O$. A solution of cobaltous acetate tetrahydrate (0.224 g, 0.90 mmol) in methanol (20 mL) was added to a solution of $L_rH_4 \cdot 4HCl \cdot H_2O$ (0.228 g, 0.30 mmol) in boiling methanol (50 mL). Lithium acetate dihydrate (0.245 g, 2.4 mmol) in methanol (25 mL) and tetrabutylammonium tetrafluoroborate (0.296 g, 0.90 mmol) in methanol (25 mL) were added; then O_2 was bubbled into the hot solution to produce a dark brown coloration. The solution was concentrated by boiling at ambient pressure to *ca.* 3 mL. Transfer of water vapor to this solution in an enclosed chamber over a period of 24 h produced a dark brown crystalline solid, which was collected and washed several times with water. Yield: 0.213 g, 62%. Addition of water to the filtrate gave a further crop of solid. Total yield: 84%.

X-ray Crystallography. Single-crystal X-ray diffraction analyses were performed on $L_rH_4 \cdot 4HCl \cdot H_2O \cdot CH_3OH \cdot C_2H_5OH$, $[L_rZn^{II}_4(OH)(CH_3CO_2)_3(CH_3OH)] \cdot 1.5CH_3OH$, and $[L_rCo^{III}_3(OH)(CH_3CO_2)_3]BF_4 \cdot 3.83H_2O$. The details of the data collection and structure refinement for each compound are given in Table 1. Accurate cell dimensions for each compound were determined from a least-squares treatment of the angular settings of 25 carefully centered reflections. Absorption corrections were numerically evaluated by Gaussian integration to a precision of 0.5%;[16] no corrections were made for extinction. The tetrahydrochloride and

---

(16) Sheldrick, G. M. *SHELX-76: A Program for Crystal Structure Determination*; University of Cambridge: Cambridge, U.K., 1976.

Co_3 structures were solved using direct methods routines;[17] the Zn_4 structure was solved from the Patterson function of SHELXS-86.[17] Parameters for the atomic scattering curves of Co and Zn, together with corrections for real and imaginary dispersion effects, were taken from ref 18; the scattering curve parameters of the remaining atoms incorporated into the SHELX-76 system were used. An analysis of variance for each structure showed no unusual features. Specific details concerning the structure analysis of each compound are given in the following text.

(a) $L_rH_4 \cdot 4HCl \cdot H_2O \cdot CH_3OH \cdot C_2H_5OH$. A crystal obtained from the slow evaporation of an acidified ethanol/methanol solution was sealed in a Lindemann glass capillary tube together with mother liquor. A full-matrix least-squares refinement procedure was employed;[16] anisotropic thermal parameters were applied to all non-hydrogen atoms in the structure. With the exception of the hydrogen atoms on O1 and O4, all the hydrogen atoms in the structure, including those associated with the water, methanol, and ethanol molecules, were clearly observed in difference maps. The H atoms on carbon and nitrogen atoms were included in the model at calculated positions using the AFIX instruction of the SHELX system.[16] The positional and isotropic thermal parameters of the hydrogen atoms on oxygen atoms were refined independently. A common isotropic thermal parameter was refined for each type of non-hydroxyl hydrogen atom.

(b) $[L_rZn^{II}_4(OH)(CH_3CO_2)_3(CH_3OH)] \cdot 1.5CH_3OH$. A colorless crystal obtained directly from the reaction mixture was sealed together with mother liquor in a Lindemann glass capillary tube. A blocked full-matrix least-squares refinement procedure was employed; anisotropic thermal parameters were applied to all of the non-hydrogen atoms except for those atoms of the methanol molecules of solvation, for which individual isotropic parameters were used. All of the H atoms in the complex, with the exception of the μ_3-hydroxide hydrogen atom and the hydroxyl hydrogen of the coordinated methanol, were observed in difference maps and included in the model at their calculated positions.

(c) $[L_rCo^{III}_3(OH)(CH_3CO_2)_3]BF_4 \cdot 3.83H_2O$. A dark red-brown monotruncated octahedral crystal, obtained from the slow diffusion of water vapor into the reaction mixture, was glued to a thin glass capillary tube using epoxy resin. A blocked full-matrix least-squares refinement procedure was employed. Initially the structure was treated as an ordered Co_3 species. Electron density of approximately 5.2 e Å^{-3} was observed in difference maps calculated at the later stages of the refinement *ca.* 2.0 Å from the μ_3-hydroxide and each of the L_r^{4-} donor atoms of the vacant nucleation compartment; this was interpreted as cation disorder. Treating the electron density as a partially occupied cobalt atom[19] and including the occupancy factors of all the cobalt atoms as independent parameters in the refinement resulted in the value of the residual index R falling from 0.112 to 0.076 at convergence; the summation of the cobalt occupancies was found to be equal to 3.04(2). The disorder appeared to be such that the cation framework could be replaced in the lattice by several other orientations without substantial alteration to the crystal packing; this would account for the partially occupied cobalt atom observed in the "vacant" site. Only one cation orientation, which is the major contributor to the structure and is the Co_3 species represented in Figure 4, was fully discernible from the data. The other cation orientations contributing to the structure could not be observed but are required to have the same chemical C_s symmetry (two different types of bridging acetates in 1:2 proportions, L_r^{4-} donor atoms coordinating in *mer,fac,mer* geometries) to remain consistent with the ^1H and ^{13}C NMR spectra. Attempts to further model the disorder of the ligand framework proved unsuccessful; consequently, all the "light" atoms of the cation (*viz.* L_r^{4-}, acetate, and hydroxyl atoms) were treated as being fully occupied. The largest peak in the residual electron density distribution (1.09 e Å^{-3}) was located within bonding distance of the least occupied cobalt atom and almost certainly corresponded to a structural fragment of a coordinated acetate, but could not be definitively modeled. Anisotropic thermal parameters were applied to all of the cobalt atoms and all of the non-hydrogen atoms of the major contributor cation. All of the H atoms in the cation associated with carbon atoms and the three coordinating amine nitrogens were clearly evident in the difference maps and were included in the model at calculated positions. A common isotropic thermal parameter was employed for each different type of hydrogen atom in the complexes, *viz.* methyl, methylene, aromatic, acetate, and amine. The hydrogen atom of the μ_3-hydroxide was observed in difference maps calculated at the later stages of the refinement and was included in the model at the positional parameters observed in the difference maps; its isotropic thermal parameter was fixed at 0.100 Å^2. A lattice water molecule within hydrogen-bonding distance of the μ_3-hydroxide (O···O, 2.78(2) Å) was assigned an occupancy factor which was complementary to that of the "fourth" cobalt atom to prevent impossible Co–O interactions. Individual isotropic thermal parameters were refined for all lattice water molecules. The BF_4^- anion was disordered over two sites: the complementary fractional populations of these sites were included as variables in the refinement; the final values were 0.612(6) and 0.388(6). Each BF_4^- site was constrained to a regular tetrahedral geometry with a common B–F distance, which was included as a parameter in the refinement [1.27(3) Å at convergence]. An isotropic thermal parameter was refined for the boron atom of the more populous BF_4^- site. The isotropic thermal parameter of the other B atom site was fixed at 0.150 Å^2. A common isotropic thermal parameter was refined for the fluorine atoms of both BF_4^- anion sites.

Physical Measurements. ^1H and ^{13}C NMR spectra were recorded on JEOL FX 90, JEOL FX 400, and Varian Unity 300 spectrometers. Infrared spectra were recorded as KBr disks on a JASCO A 302 spectrophotometer.

Microanalyses were performed by the University of Otago Microanalytical Service, P.O. Box 56, Dunedin, New Zealand, and Analytische Laboratorien, Engelskirchen, Germany.

Acknowledgment. We thank the Australian Research Grants Scheme for support.

Supplementary Material Available: Tables S-1–S-4, listing H atom parameters, anisotropic thermal parameters, complete interatomic distances and bond angles, and least-squares planes for $L_rH_4 \cdot 4HCl \cdot H_2O \cdot CH_3OH \cdot C_2H_5OH$, Tables S-5–S-8, listing the corresponding data for $[L_rZn^{II}_4(OH)(CH_3CO_2)_3(CH_3OH)] \cdot 5CH_3OH$, and Tables S-9–S-13 listing all refined atomic coordinates, H atom parameters, anisotropic thermal parameters, complete interatomic distances and bond angles, and least-squares planes for $[L_rCo^{III}_3(OH)(CH_3CO_2)_3]BF_4 \cdot 3.83\ H_2O$ (31 pages). Ordering information is given on any current masthead page.

---

(17) Sheldrick, G. M. SHELX-76: A Program for Crystal Structure Determination. In *Crystallographic Computing 3*; Sheldrick, G. M., Kruger, C., Goddard, R., Eds.; Oxford University Press: Oxford, U.K., 1985; p 175.

(18) Ibers, J. A., Hamilton, W. C., Eds. *International Tables for X-ray Crystallography*; Kynoch: Birmingham, U.K., 1974; Vol. IV.

(19) We are grateful to a reviewer who suggested we model the cation disorder in this manner.